

# The effect of ordered submonolayer oxygen films on the electrical resistance of thin tungsten plates

A. A. Mitryaev, E. M. Kogan, V. V. Ustinov, and D. Z. Khusainov

*Institute of Physics, Academy of Sciences of the Ukrainian SSR, Kiev*

*Institute of Metal Physics, Ural Scientific Center of the Academy of Sciences of the USSR, Sverdlovsk*

(Submitted 13 April 1984)

Zh. Eksp. Teor. Fiz. **87**, 1765–1773 (November 1984)

Features of the classical size effect have been investigated in the electrical resistance of tungsten plates, on one of the surfaces of which oxygen atoms are adsorbed. A direct correlation was observed between the behavior of the electrical resistance and the magnetoresistance of the plates under static skin-effect conditions, which indicates the significant role of umklapp processes on reflection of electrons from a surface with an adsorbed layer. It is shown that the main features of the dependence of the resistance of tungsten plates on the coverage of the surface by oxygen atoms can be explained by taking account of the competition between multichannel specular reflection processes and conduction electron scattering processes due to partial buildup of regular two-dimensional structures arising on the surface.

## INTRODUCTION

Multichannel specular reflection of conduction electrons from the surface is a characteristic of metals with a complicated dispersion law for the carriers and an atomically clean surface, or when an ordered system of adsorbed atoms exists on the perfect faces of the specimen.<sup>1–4</sup> Multichannel specular reflection processes (or, otherwise, umklapp processes at the surface<sup>5</sup>) appreciably affect the dynamics of carriers in the surface layer and lead to a number of new effects.<sup>6,8</sup> In particular, the dissipation of electron momentum in umklapp processes at the surface can play an important part in different aspects of charge transfer processes near the boundaries of conductors, among them the classical size effect in electrical resistivity.<sup>9</sup>

Traditional methods of studying the size effect<sup>10</sup> are based on measurements of the resistance of a specimen as a function either of specimen thickness or of temperature, on which the electron mean free path depends. However, the possible uncontrolled change in the details of the atomic structure of a surface on going from specimen to specimen or on changing the temperature over wide limits, restricts the applicability of these methods.

One of the possible means of studying the connection between the atomic structure of the boundary and the nature of the reflection of conduction electrons consists in a controlled change in the state of the surface over wide limits on adsorbing foreign atoms on the surface of the specimen. Such a connection was studied in tungsten,<sup>11</sup> using two independent methods: low energy electron diffraction and the static skin effect. As a result, a correlation was established between features of the symmetry of the surface lattice of adsorbed atoms and the behavior of the magnetoresistance of tungsten under static skin effect conditions.

In the present work, the effect of adsorption of submonolayer oxygen films on the electrical resistance of thin tungsten plates oriented in the (110) plane was studied under classical size-effect conditions. The aim of the work was the study of the influence of ordered surface structures on the

magnitude of the electrical resistivity of tungsten plates, based on a comparison of the results of the size effect with results on the static skin effect. A relatively simpler theoretical description of the classical size effect enable the results obtained to be interpreted qualitatively and for them to be illustrated by numerical calculations.

## EXPERIMENTAL METHOD

Studies of the size effect in single-crystal tungsten plates were carried out in a glass vacuum apparatus, the lower (“cold”) part of which, with the specimen under investigation, was in a metal cryostat at liquid helium temperature. The specimen in the shape of a plate with dimensions  $9 \times 2 \times 0.1$  mm was cut out, in a [100] direction, from a single-crystal tungsten ingot with resistance ratio  $\rho(300 \text{ K})/\rho(4.2 \text{ K}) \approx 10^5$ . The surface of the plate in the (110) plane, was treated in the standard way<sup>11–13</sup> and maintained under high vacuum conditions at  $10^{-9}$ – $10^{-10}$  mm Hg. The specimen was in thermal contact with the external helium bath through 1.5 mm diameter molybdenum leads. A measuring current  $J$  (0.1–2 A) was applied to the specimen through the leads, as was the current for high-temperature cleaning of the crystal surface.

The plate being studied had three  $1 \times 1$  mm projections along the long edge. A differential tungsten-rhenium thermocouple was welded to the central projection with a spot welder. Calibration in the temperature range 1000–2500 K was carried out by means of an optical pyrometer, and it was assumed that in the temperature range 4.2–1000 K the dependence of the thermocouple signal on temperature is linear. The two projections on the edges of the plate were used as potential contacts in a four-point scheme for measuring resistance. The sensitivity of the measuring system was  $5 \times 10^{-10}$  V.

A pressure gauge, a titanium getter pump and an oxygen source were housed in the upper (“hot”) part of the experimental apparatus. Oxygen was obtained from thermal dissociation of CuO powder, contained in a thin-walled 2

mm diameter, 30 mm long platinum tube.

A superconducting magnet was immersed in the helium bath, with which a steady magnetic field of strength up to 20 kOe could be provided to achieve the static skin effect regime.

### EXPERIMENTAL RESULTS

An automatically recorded trace of the time ( $t$ ) dependence of the signal  $\Delta U$  from the potential contacts for a thin single-crystal tungsten plate is shown in Fig. 1. The start of the trace was preceded by high-temperature heating of the crystal, in order to obtain an atomically clean surface, and cooling of the specimen to  $T = 4.2$  K. Sections 1 and 4 corresponds to the time dependence of the signal from the potential contacts with the measuring current through the specimen switched off. The residual gas pressure in the "warm" section of the vacuum apparatus was  $P = 10^{-10}$  mm Hg. Sections 2 and 3 correspond to the trace on switching on the measuring current through the specimen. At the instant  $t_0$  the oxygen source was connected and the time for establishing an equilibrium pressure  $P = 1 \times 10^{-5}$  mm Hg in the warm part of the vacuum apparatus was about 10 s. It can be seen from Fig. 1 that the deposition of oxygen on the atomically clean surface of the plate leads to an increase in electrical resistance by a factor of one and a half (section 3). Subsequent cleaning of the crystal surface to the atomically clean state on disconnecting the oxygen source enabled the experiment with adsorbed oxygen to be repeated many times. The potential signal  $\Delta U$  for the specimen in the static skin effect regime, under the same experimental conditions as for the  $\Delta U(t)$  curve traced in Fig. 1, showed that deposition of oxygen on the atomically clean surface of the plate leads to a threefold increase in magnetoresistance. The magnetic field  $H = 10$  kOe lay in the plane of the plate and was perpendicular to the direction of the measuring current  $J$ .

Figure 2 shows a set of plots of the electrical resistivity  $\rho$  of a tungsten plate as a function of the annealing temperature  $T_{\text{ann}}$  of the oxygen film on the surface. The parameter of the  $\rho(T_{\text{ann}})$  curves is the time  $t$  for the adsorption of oxygen on the surface of the plate. Oxygen was adsorbed on the surface

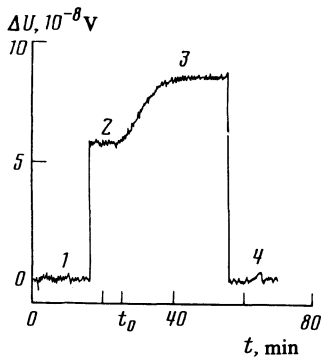


FIG. 1. Automatic trace of the dependence of the signal  $\Delta U$  from the potential contacts of a thin single-crystal plate of tungsten on time  $t$  in the absence of a magnetic field,  $n \perp (110)$ ,  $J \parallel [100]$ ,  $T = 4.2$  K. Sections 1 and 4 correspond to the trace when the current through the specimen is switched off, sections 2 and 3 to the measuring current  $J$  being switched on. The oxygen source is connected at the instant  $t_0$ .

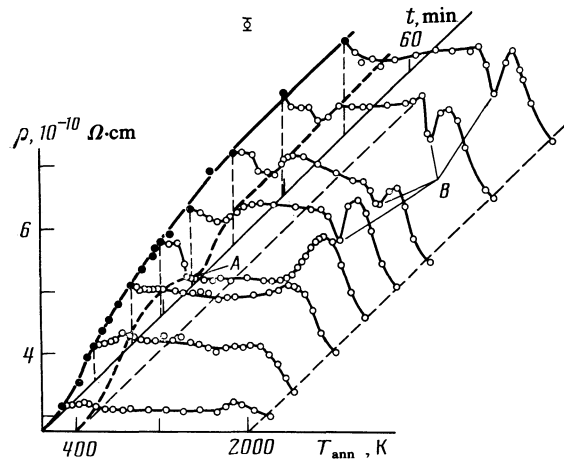


FIG. 2. The dependence of the resistivity  $\rho$  of a tungsten plate on annealing temperature  $T_{\text{ann}}$  for different times  $t$  for adsorption of oxygen on the surface of the specimen.

which had been cleaned to the atomically clean state and cooled to a temperature  $T = 4.2$  K. The successive points on the  $\rho(T_{\text{ann}})$  curves were obtained on heating the crystal to the corresponding  $T_{\text{ann}}$  and cooling to 4.2 K for measuring  $\rho$ . It can be seen from Fig. 2 that  $\rho$  for  $T_{\text{ann}} = 2000$  K is equal to the electrical resistivity of the plate with an atomically clean surface, i.e. for  $T_{\text{ann}} > 2000$  K the oxygen is completely desorbed from the tungsten surface.<sup>14</sup> After cooling the crystal to  $T = 4.2$  K and depositing a new portion of oxygen on the surface, annealing of the film and measuring of the  $\rho(T_{\text{ann}})$  dependence were repeated.

A set of plots of the magnetoresistance (the static skin-effect electrical resistivity)  $\rho_{\text{sse}}$  of the specimen as a function of the annealing temperature  $T_{\text{ann}}$  is shown in Fig. 3 for different times of oxygen adsorption on the surface. The conditions of the experiment when depositing oxygen were the same when obtaining the results shown in Fig. 2. The distin-

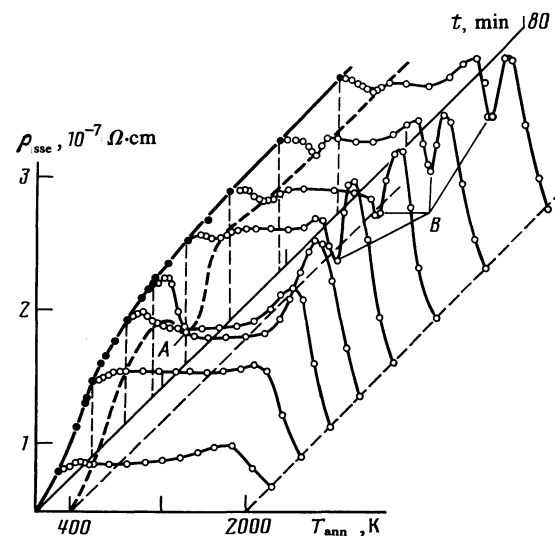


FIG. 3. The dependence of magnetoresistance  $\rho_{\text{sse}}$  of a specimen on annealing temperature  $T_{\text{ann}}$  for different times  $t$  for adsorption of oxygen on the surface,  $H = 10$  kOe,  $J \parallel [100]$ , H1J, H1n.

guishing feature of this experiment was the presence of the magnetic field lying in the plane of the plate and producing the static skin effect conditions. According to Lutsishin *et al.*,<sup>11</sup> the first minimum in the  $\rho_{sse}(t)$  curve for  $T_{ann} = 400$  K, shown by the thick dashed line, corresponds to the maximum of the  $(2 \times 1)$  structure and the subsequent minimum corresponds to the greatest development of the  $(2 \times 2)$  structure. As in Lutsishin *et al.*,<sup>11</sup> we did not obtain a further reduction in the  $\rho_{sse}(t)$  dependence, which is associated with a reduction in the oxygen sticking probability in the region of the covering thickness  $\Theta > 0.8$  at a substrate temperature  $T = 4.2$  K (Ref. 15). It can be seen from Figs. 2 and 3 that the behavior of the series of resistivity  $\rho(T_{ann})$  and magnetoresistance  $\rho_{sse}(T_{ann})$  curves is the same for the same surface oxygen concentration.

We note that for annealing temperatures  $T > 500$  K desorption of oxygen from the crystal surface takes place with desorption products  $WO_2$  and  $WO_3$ , while for temperatures  $T > 1500$  K it is in the form of the atomic phase.<sup>14</sup> As the oxygen concentration is reduced, for increasing  $T_{ann}$ , the  $\rho(T_{ann})$  and  $\rho_{sse}(T_{ann})$  curves repeat the behavior of the  $\rho(t)$  and  $\rho_{sse}(t)$  curves obtained for  $T_{ann} = 400$  K (the dashed curves in Figs. 2 and 3), while the sequence of the corresponding minima and maxima occur in the reverse order. There are, for example, two routes for reaching the resistance and magnetoresistance minima corresponding to the covering thickness  $\Theta \sim 0.5$  and to the maximum development of the ordered  $(2 \times 1)$  structure on the surface. The first possibility is realized by the deposition of oxygen up to a covering  $\Theta \sim 0.5$  and annealing to a temperature  $T_{ann} = 400$  K (point *A* in Figs. 2 and 3). The second route consists of depositing oxygen to a coverage  $\Theta > 0.5$  and subsequent annealing and desorption of oxygen until the characteristic minimum appears in the  $\rho(T_{ann})$  and  $\rho_{sse}(T_{ann})$  plots.

## INTERPRETATION OF THE RESULTS AND CONCLUSIONS

From the identical nature of the features of the behavior of the electrical resistivity  $\rho$  and magnetoresistance  $\rho_{sse}$ , together with earlier<sup>11</sup> deductions of a correlation between the  $\rho_{sse}$  extrema and the formation of ordered structures on a tungsten surface, it can be asserted that the nonmonotonic nature of the dependence of  $\rho$  on the number of adsorbed atoms on the surface is a consequence of an ordering process at the boundary. According to earlier results,<sup>11</sup> the adsorption of oxygen atoms on a (110) tungsten face occurs in such a way that for a relative oxygen atom covering concentration of 1/2 and 3/4 on the face at a given temperature, ordered lattices can be formed with the structures  $p(2 \times 1)$  and  $(2 \times 2)$ , respectively. The impurity lattice on the surface is characterized by the existence of short range order, which is revealed in clearly defined diffraction patterns of low energy electrons reflected from the surface, and by the absence of long range order, which is connected with unavoidable surface defects of various kinds (growth steps, roughness, etc).

Because of the absence of long-range order on the surface of the face, the reflection of conduction electrons from the crystal boundary having adsorbed atoms can be described,<sup>16</sup> with the help of linear boundary conditions for the

electron distribution function, expressed in integral form by a distribution function for electrons reflected at the boundary ( $z = 0$ ) through an incident distribution function and a probability  $W_{kk'}$  of an electron transition from state  $k'$  to state  $k$  per unit collision with the scattering surface.<sup>17</sup> The existence of short range order leads then to the probability  $W_{kk'}$  having a sharp maximum, corresponding to the conditions for Bragg reflection of electrons from the surface lattice.

In the case of an arbitrary concentration of adsorbed atoms on the surface, there is additional disorder associated with the random nature of the buildup of the sublattices mentioned above. The disorder leads to the usual surface scattering which makes, together with multichannel specular reflection processes, a contribution to the probability  $W_{kk'}$ . The relative insensitivity of both types of scattering depends appreciably on the concentration of impurity deposited. To a first Born approximation, the scattering probability  $W_{kk'}$  is expressed through the interaction potential  $V$  of an electron with the adsorbed atoms.<sup>17</sup> Writing  $V$  in the form of a sum of potentials  $\Phi$  of the scattering adsorbed atoms, localized at sites  $\mathbf{R}_n$  of the surface lattice, and using the property of translational symmetry of the electron wave functions in a crystal with an ideal surface, the matrix elements  $V_{kk'}$  can be expressed in terms of the elements  $\Phi_{kk'}$ , and the probability  $W_{kk'}$  can be written in the following way:

$$W_{kk'} = \frac{2L}{v_k^z} \frac{2\pi}{\hbar} |\Phi_{kk'}|^2 NS(\boldsymbol{\kappa} - \boldsymbol{\kappa}') \delta(\epsilon_k - \epsilon_{k'}), \quad (1)$$

where  $v_k^z$  is the modulus of the electron velocity vector along the normal  $z$  to the surface,  $L$  is the plate thickness,  $N$  the number of sites of the surface crystal plane and  $\boldsymbol{\kappa}$  is the tangential component of the wave vector  $\mathbf{k}$ ,

$$S(\boldsymbol{\kappa}) = \frac{1}{N} \left\langle \sum_{n_1, n_2} \exp\{-i\boldsymbol{\kappa}(\mathbf{R}_{n_1} - \mathbf{R}_{n_2})\} \right\rangle \quad (2)$$

is the surface structure factor; the angular brackets indicate averaging over the scattering potential configurations.

We assume that the adsorbed atoms fill completely the sublattice  $i$  and partially, with relative concentration  $c_j$ , the sublattice  $j$ , with their distribution being random over the sublattice being built up.

For describing the process of adsorption of oxygen atoms on a (110) face of tungsten,<sup>11</sup> we distinguish three sublattices, represented in Fig. 4 by the numbers 1, 2 and 3. Adsorption of oxygen on this face takes place in the following way: sublattice 1 is filled up at first, then cells of lattice 2 are filled up, and when positions 1 and 2 have been filled, the third sublattice is filled. Going from summation over sites in Eq. (2), after averaging, to summation over vectors  $\mathbf{g}$  of the reciprocal lattice surface of the (110) face, for each of the three stages described above, we obtain-

$$\begin{aligned} S_1(\mathbf{q}) &= \frac{1}{2} c_1(1-c_1) + \frac{\pi^2 c_1^2}{s_0} \sum_{\mathbf{g}} \left[ \delta(\mathbf{q}-\mathbf{g}) + \delta\left(\mathbf{q}-\mathbf{g}-\frac{\mathbf{g}_1}{2}\right) \right]; \\ S_2(\mathbf{q}) &= \frac{1}{4} c_2(1-c_2) + \frac{\pi^2}{4s_0} \sum_{\mathbf{g}} \left[ (2+c_2)^2 \delta(\mathbf{q}-\mathbf{g}) \right] \end{aligned} \quad (3)$$

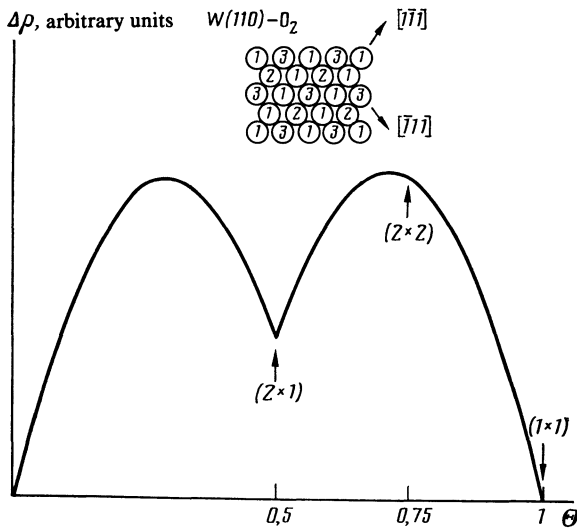


FIG. 4. The theoretical dependence of the contribution  $\Delta\rho$  of adsorbed oxygen to the electrical resistivity (in arbitrary units) of a tungsten plate on the degree of covering  $\Theta$  for values of the parameters  $r_{1/2} = 0.6$  and  $R_{3/4} = 1.2$ . The inset shows the arrangements of the lattices formed by oxygen atoms on a (110) face of tungsten. The circles with the number 1 correspond to the  $p(2 \times 1)$  structure; circles with the number 2 form the lattice filled in on going from the  $p(2 \times 1)$  to the  $(2 \times 2)$  structure and those numbered 3 form the lattice filling up the  $(2 \times 2)$  structure up to the  $p(1 \times 1)$  structure which possesses the symmetry of the substrate face.

$$+ (2 - c_2)^2 \delta \left( \mathbf{q} - \mathbf{g} - \frac{\mathbf{g}_1}{2} \right) \quad (4)$$

$$+ c_2^2 \delta \left( \mathbf{q} - \mathbf{g} - \frac{\mathbf{g}_2}{2} \right) + c_2^2 \delta \left( \mathbf{q} - \mathbf{g} - \frac{\mathbf{g}_1}{2} - \frac{\mathbf{g}_2}{2} \right) \Big];$$

$$S_3(\mathbf{q}) = \frac{1}{4} c_3 (1 - c_3) + \frac{\pi^2}{4s_0} \sum_{\mathbf{g}} \left\{ (3 + c_3)^2 \delta(\mathbf{q} - \mathbf{g}) + (1 - c_3)^2 \times \left[ \delta \left( \mathbf{q} - \mathbf{g} - \frac{\mathbf{g}_1}{2} \right) + \delta \left( \mathbf{q} - \mathbf{g} - \frac{\mathbf{g}_2}{2} \right) + \delta \left( \mathbf{q} - \mathbf{g} - \frac{\mathbf{g}_1}{2} - \frac{\mathbf{g}_2}{2} \right) \right] \right\}, \quad (5)$$

where  $\mathbf{g}_1$  and  $\mathbf{g}_2$  are the basic vectors of the reciprocal two-dimensional lattice and  $s_0$  is the area of the elementary cell of the (110) face of tungsten.

From the solution of the kinetic equation for the distribution function with the boundary conditions, the conductivity of the plate can be calculated, and its dependence on the degree of filling of the monolayer of adsorbed atoms can be found. Since the walls of the lower part of the vacuum apparatus (about 50 cm long), in which the specimen was placed, was cooled to  $T = 4.2$  K, it could be expected that deposition of oxygen only took place on the one side of the plate facing the oxygen source. For simplicity we will assume that the other side of the plate, with a state which evidently did not change during deposition of oxygen on the first face, scatters diffusely. With this assumption we can write the conductivity of the plate in explicit form in terms of the scattering probability  $W_{kk'}$  for electrons at the surface studied.<sup>18</sup> In view of the assumed weakness of electron scattering by adsorbed atoms, the resistivity  $\rho$  of the plate can then be represented in the form  $\rho = \rho_0 + \Delta\rho$ , where  $\rho_0$  is the

part independent of scattering at the adsorbing face, while  $\Delta\rho$  depends in the following way on  $W_{kk'}$ :

$$\Delta\rho \sim \sum_{kk'} (v_k^x)^2 v_k^z W_{kk'} \left[ 1 - \exp \left( -\frac{L}{\tau v_k^z} \right) \right]^2 \times \left[ 1 - \frac{v_k^x}{v_k^z} \frac{1 - \exp(-L/\tau v_k^z)}{1 - \exp(-L/\tau v_k^z)} \right] \delta(\epsilon_k - \epsilon_F). \quad (6)$$

Here  $\tau$  is the mean free time limited by bulk scattering mechanisms and  $\epsilon_F$  is the Fermi energy. Substituting the expressions of Eqs. (1)–(5) into Eq. (6), we obtain the basic relations for the analysis of the relative changes in resistance on changing the state of the surface studied.

An analysis has been carried out<sup>11</sup> of possible electron transitions on reflection from a (110) tungsten face with regular  $p(2 \times 1)$  and  $(2 \times 2)$  structures. The contribution to the resistivity for incomplete buildup of the structures will come from both umklapp processes and incoherent scattering processes, described by the first terms of Eqs. (3)–(5). While the  $p(2 \times 1)$  structure (sublattice 1 in Fig. 4) is being formed, the contribution  $\Delta\rho_1$  will be determined, first of all, by the narrow regions of phase space where umklapp processes are possible between the electron “jack” and the hole “octahedron” and also between the hole “ellipsoids” and the residual sections of the Fermi surface of tungsten through the vector  $\mathbf{g}_{1/2}$  and multiples of it, and, secondly, by incoherent scattering, in the process of which an electron can go to an arbitrary point of the Fermi surface. Extracting the dependence of  $\Delta\rho_1$  on concentration  $c_1$  in explicit form, we obtain

$$\Delta\rho_1 = 4c_1(1 - c_1)\Delta\rho_{inc} + c_1^2\Delta\rho_{1/2}, \quad (7)$$

where the coefficients  $\Delta\rho_{inc}$  and  $\Delta\rho_{1/2}$ , which describe the intensity of incoherent scattering and umklapp scattering through the vector  $(\mathbf{g}_{1/2} + \mathbf{g})$ , are expressed only in terms of characteristics of the Fermi surface and the matrix elements of the scattering potential of the adsorbed atoms, and depend on the parameters  $\tau$  and  $L$ . Because of the small region of phase space where umklapp processes are possible due to the  $p(2 \times 1)$  structure, the magnitude of  $\Delta\rho_{1/2}$  clearly does not exceed  $\Delta\rho_{inc}$  so that the ratio  $r_{1/2} \equiv \Delta\rho_{1/2}/\Delta\rho_{inc} < 1$ .

On formation of the  $(2 \times 2)$  structure (the combination of sublattices 1 and 2 in Fig. 4), umklapp scattering becomes possible by the vectors  $\mathbf{g}_{1/2} + \mathbf{g}$ ,  $\mathbf{g}_{2/2} + \mathbf{g}$  and  $\mathbf{g}_{1/2} + \mathbf{g}_{1/2} + \mathbf{g}$  between the hole “octahedron” of the Fermi surface and the electron “jack.” Then, consistent with Eq. (4), we can write

$$\Delta\rho_2 = 2c_2(1 - c_2)\Delta\rho_{inc} + (1 - c_2)\Delta\rho_{1/2} + c_2^2\Delta\rho_{1/2}, \quad (8)$$

where the parameter  $\Delta\rho_{3/4}$  describes the intensity of the transitions designated above. The most effective of them are umklapp scattering by the vector  $(\mathbf{g}_1 + \mathbf{g}_2)/2$ . In view of the fact that umklapp scattering by such vectors is possible in a region of appreciable volume in phase space, the magnitude of  $\Delta\rho_{3/4}$  is comparable with  $\Delta\rho_{inc}$  and the ratio  $r_{3/4} \equiv \Delta\rho_{3/4}/\Delta\rho_{inc} \sim 1$ .

At the third and last stage in the formation of an oxygen monolayer, when the reestablishment of the initial symmetry of the (110) face takes place, we obtain according to Eq. (5)

$$\Delta\rho_3 = 2c_3(1 - c_3)\Delta\rho_{inc} + (1 - c_3)^2\Delta\rho_{1/2}. \quad (9)$$

In obtaining Eqs. (7)–(9) we have considered the umklapp processes through vectors  $g$  of the reciprocal lattice are practically forbidden.

We will not quote here the cumbersome expressions for the coefficients  $\Delta\rho_{inc}$ ,  $\Delta\rho_{1/2}$  and  $\Delta\rho_{3/4}$ , since the determinants of their matrix elements of the scattering potential of adsorbed atoms are unknown, and we will consider these quantities as adjustable parameters. Since we are only interested in relative changes in the value of  $\Delta\rho$ , two dimensionless quantities can be used as parameters: the ratios  $r_{1/2}$  and  $r_{3/4}$ . According to Eqs. (7)–(9), the dependence of  $\Delta\rho$  on the degree of covering  $\theta$  takes the form  $\Delta\rho/\Delta\rho_{inc} = F(\theta)$  where

$$F(\theta) = \begin{cases} 8\theta(1-2\theta) + 4r_{1/2}\theta^2, & \theta \leq 1/2 \\ 4(2\theta-1)(3-4\theta) + r_{1/2}(3-4\theta) + 4r_{3/4}(2\theta-1)^2, & 1/2 \leq \theta \leq 3/4 \\ 8(4\theta-3)(1-\theta) + 16(1-\theta)^2 r_{3/4}, & 3/4 \leq \theta \leq 1 \end{cases} \quad (10)$$

The behavior of  $F(\theta)$  with an appropriate choice of the parameters  $r_{1/2}$  and  $r_{3/4}$  correctly provides all the main features of the experimentally observed dependences of  $\Delta\rho$  on annealing temperature or time for deposition of oxygen atoms. In fact, during the formation of the  $p(2 \times 1)$  structure (see Fig. 2) the surface contribution to the resistivity  $\Delta\rho$  increases to some maximum value  $\Delta\rho_{max}^{(1)}$  and then decreases, reaching a value  $\Delta\rho_{min}$  different from zero, which amounts to about half  $\Delta\rho_{max}^{(1)}$ . The function  $F(\theta)$  behaves similarly at  $r_{1/2} \approx 0.6$ . During the process of formation of the  $(2 \times 2)$  structure of further increase in resistivity  $\Delta\rho$  takes place up to a value  $\Delta\rho_{max}^{(2)}$ , which coincides approximately with  $\Delta\rho_{max}^{(1)}$ . The function  $F(\theta)$  behaves in the same way for  $r_{3/4} \approx 1.2$ . The behavior of  $F(\theta)$  for  $r_{1/2} = 0.6$  and  $r_{3/4} = 1.2$  is shown in Fig. 4.

The results of the comparative study of the effect of ordered oxygen films on the electrical resistivity and magnetoresistance of thin tungsten plates, shown in Figs. (2) and (3), and also the theoretical treatment carried out, are thus evidence of the sensitivity of the size effect in electrical resistivity to umklapp processes at the surface. The difference in the sensitivity of the size effect and of the static skin effect to adsorbed oxygen is related to the different role of bulk scattering. Under static skin effect conditions the bulk conductivity is  $10^2$ – $10^3$  times less than that of the surface,<sup>11</sup> while

under the usual size effect conditions the bulk scattering “shunts” the electron-surface scattering.

The nature of the features found in studying the size effect in electrical resistivity agree with the relationships obtained earlier when studying the static skin effect, and can be explained by taking account of scattering and the multichannel character of the reflection of current carriers from a surface having a lattice of adsorbed atoms.

The authors are grateful to O. A. Panchenko for his interest in the work and for discussion of the results.

<sup>1</sup>A. F. Andreev, Usp. Fiz. Nauk, **105**, 113 (1971) [Sov. Phys. Usp. **14**, 609 (1972)].

<sup>2</sup>R. F. Green in: Progress in the Surface Science of Solids [Russian translation] Mir, Moscow (1977), No. 2, Chap. 8, pp. 243–279.

<sup>3</sup>V. F. Gantmakher and I. B. Levinson, Poverkhnost', No. 25 (1982).

<sup>4</sup>V. V. Ustinov, Fiz. Met. Metalloved. **52**, 709 (1981) [Phys. Met. and Metallogr. (GB) **52**, No. 4, 27 (1981)].

<sup>5</sup>R. M. More, Phys. Rev. **B9**, 392 (1974).

<sup>6</sup>V. G. Peschanskiĭ, V. Kardenas, M. A. Lur'e, and K. Yasemidis, Zh. Eksp. Teor. **80**, 1645 (1981) [Sov. Phys. JETP **53**, 849 (1981)].

<sup>7</sup>V. G. Peschanskiĭ, Umklapp processes in the surface scattering of conduction electrons, Preprint, Physicotechnical Institute, Academy of Sciences of the Ukrainian SSR, Donetsk, 81–28 (1981).

<sup>8</sup>A. A. Slutskii and A. M. Kadigrobov, Pis'ma Zh. Eksp. Teor. Fiz. **32**, 363 (1980) [JETP Lett. **32**, 338 (1980)].

<sup>9</sup>P. J. Price, IBM J. Res. Dev. **4**, 152 (1960).

<sup>10</sup>D. K. Larson, Thin Film Physics [Russian translation] Vol. 6, Mir, Moscow (1973) Ch. 2, pp. 97–170.

<sup>11</sup>P. P. Lutsishin, T. N. Nakhodkin, O. A. Panchenko, and Yu. G. Ptushinskiĭ, Zh. Eksp. Teor. Fiz. **82**, 1306 (1982) [Sov. Phys. JETP **55**, 759 (1982)].

<sup>12</sup>P. P. Lutsishin, O. A. Panchenko, and A. A. Karlamov, Zh. Eksp. Teor. Fiz. **64**, 2148 (1973) [Sov. Phys. JETP **37**, 1083 (1973)].

<sup>13</sup>A. A. Mitryaev, Fiz. Nizk. Temp. **5**, 471 (1979) [Sov. J. Low Temp. Phys. **5**, 226 (1979)].

<sup>14</sup>Yu. G. Ptushinskiĭ and B. A. Chuĭkov, Fiz. Tverd. Tela (Leningrad) **10**, 722 (1968) [Sov. Phys. Solid State **10**, 565 (1968)].

<sup>15</sup>V. S. Bosov and B. A. Chuĭkov, Ukr. Fiz. Zh. **18**, 1568 (1973).

<sup>16</sup>E. M. Kogan, Yu. N. Gornostirev, and V. V. Ustinov, Phys. Status Solidi B (1984).

<sup>17</sup>V. I. Okulov and V. V. Ustinov, Fiz. Nizk. Temp. **5**, 214 (1979) [Sov. J. Low Temp. Phys. **5**, 101 (1979)].

<sup>18</sup>V. V. Ustinov, Fiz. Met. Metalloved. **39**, 1127 (1975) [Phys. Met. and Metallogr. (GB) **39**, No. 6, 1 (1975)].

Translated by R. Berman